Calorimetric Study of the Interaction of the C2 Domains of Classical Protein Kinase C Isoenzymes with Ca^{2+} and Phospholipids†

Alejandro Torrecillas,‡ José Laynez,§,|| Margarita Menéndez,§ Senena Corbalán-García,‡ and Juan C. Gómez-Fernández*,‡

Departamento de Bioquímica y Biología Molecular (A), Facultad de Veterinaria, Universidad de Murcia, Apartado de Correos 4021, E-30080-Murcia, Spain, and Instituto de Química-Física "Rocasolano", Consejo Superior de Investigaciones Científicas (CSIC), Madrid, Spain

Received May 21, 2004; Revised Manuscript Received July 15, 2004

ABSTRACT: The affinities of Ca^{2+} and anionic lipid vesicles from the C2 domains of classical protein kinase C subfamily (α, βII, and γ) were studied using isothermal titration calorimetry (ITC). In addition, the thermal stability of these C2 domains in the presence of different ligand concentrations was analyzed using differential scanning calorimetry (DSC). These three closely related C2 domains bind Ca^{2+} in a similar way, demonstrating the presence of two sets of sites. The first set of sites binds one Ca^{2+} ion exothermically with similar high affinity for the three proteins (K_d around 1 μM), while the second set of sites binds endothermically approximately two Ca^{2+} ions with lower affinity, which varies for each C2 domain: 22.2 μM for the PKCα−C2 domain, 17.2 μM for the PKCβII−C2 domain, and 4.3 μM for the PKCγ−C2 domain. In the absence of Ca^{2+}, the three C2 domains showed a weak interaction with vesicles containing anionic phospholipids. However, in the presence of a saturating Ca^{2+} concentration, the C2 domains increased their affinities for the anionic lipid vesicles. In all cases, the C2 domains bound the vesicles exothermically and with similar affinities. A DSC thermal stability study of the C2 domains in the presence of Ca^{2+} and anionic lipids provided further information about this protein−ligand interaction. The presence of increasing Ca^{2+} concentrations was matched by an increase in the T_m in all cases, which was even greater in the presence of anionic lipid vesicles. The extent of the change in T_m differed for each C2 domain, reflecting the differing effect of the ligands bound during the protein stabilization. Denaturation of the C2 domains was irreversible both in the absence and in the presence of ligands, although the thermograms were not kinetically controlled. The dependence of the T_m on the Ca^{2+} concentration indicates that the protein stabilization observed by DSC primarily reflects the saturation by the cation of the low-affinity set of sites.

Protein kinase C (PKC)[1] is a large family of phospholipid-dependent serine/threonine kinases, which is activated by many extracellular signals and plays a critical role in several signaling pathways in the cell (*1*−*3*). The mammalian isoenzymes have been grouped into three subfamilies according to their enzymatic properties (*4*−*5*). The first group, called classical isoenzymes, includes PKCα, βI, βII, and γ, all of which contain the conserved C1 and C2 domains in the regulatory region. These isoenzymes are regulated by diacylglycerol (DAG) and, cooperatively, by Ca^{2+} and acidic phospholipids, especially phosphatidylserine (PS). The second group, the novel PKCs (δ, ε, η, and θ), also contain C1 and C2 motifs, although they are located in reverse order from those of the classical isoenzymes and are activated by phospholipid and diacylglycerol binding in a Ca^{2+}-independent manner. Finally, the atypical group of PKC isoenzymes (ζ, ι, and λ) contain an atypical C1 domain and are not regulated by DAG or Ca^{2+} (*2*, *6*−*7*).

C2 domain is a regulatory sequence motif that contains approximately 130 amino acid residues and is found in a large variety of proteins involved in intracellular signal transduction and membrane trafficking. In these processes, the C2 domain mediates protein recruitment by the phospholipid membranes (*8*−*9*). All of the C2 domains are composed of a stable β sandwich with flexible loops on top

† This work was supported by Grants BMC2002-00119 from Dirección General de Investigación, Ministerio de Ciencia y Tecnología (Spain) and PI-35/00789/FS/01 from Fundación Séneca (Comunidad Autónoma de Murcia, Spain). A.T. is a recipient of a fellowship from Fundación Cajamurcia (Murcia, Spain). S.C.-G. belongs to "Ramón y Cajal Programme" supported by Ministerio de Ciencia y Tecnología and the University of Murcia.

* To whom correspondence should be addressed. Telephone: +34-968-364766. Fax: +34-968-364766. E-mail: jcgomez@um.es.

‡ Universidad de Murcia.

§ Consejo Superior de Investigaciones Científicas (CSIC).

|| Deceased December 25th, 2002.

[1] Abbreviations: $C_{p,max}$, heat capacity at T_m; DAG, diacylglycerol; DSC, differential scanning calorimetry; EGTA, ethylene glycol-bis(β-aminoethyl ether)-*N*,*N*,*N*′,*N*′-tetraacetic acid; FTIR, Fourier transform infrared spectroscopy; ICP-OE, inductively coupled plasma optical emission spectroscopy; IPTG, isopropyl-1-thio-β-D-galactopyranoside; ITC, isothermal titration calorimetry; K_d, dissociation constant; *n*, number of bound ligand molecules; PI3K, phosphatidylinositol-3-kinase; PKC, protein kinase C; PMSF, phenylmethylsulfonyl fluoride; POPC, 1-palmitoyl-2-oleoyl-*sn*-glycero-3-phosphocholine; POPS, 1-palmitoyl-2-oleoyl-*sn*-glycero-3-phospho-L-serine; SUV, small unilamellar vesicle; T_m, the maximum transition temperature; $T_{1/2}$, half-bandwidth transition temperature; ΔC_p, denaturation heat capacity change; ΔH, enthalpy change; ΔH_{vH}, van't Hoff enthalpy change; ΔS, entropy change.

10.1021/bi0489659 CCC: $27.50
Published on Web 08/25/2004

and at the bottom, as seen from the crystal structures of the C2 domains from synaptotagmin I (*10*−*12*), phospholipase C-δ (*13*−*14*), phospholipase A2 (*15*−*17*), PKCβI (*18*), PKCδ (*19*), PKCα (*20*−*22*), PKCϵ (*23*), PTEN (*24*), and PI3K (*25*). In the case of synaptotagmin I, the two phospholipases, PKCβI, and PKCα, the C2 domain contains a Ca^{2+}-binding site, which is formed by a pair of loops located on one side of the domain. The C2 domains can adopt two topologies, called type I and type II, which only differ in a circular change of the amino and carboxi termini with respect to the tertiary fold (reviewed in refs *26* and *27*). In the case of PKC, the C2 domains of classical isoenzymes have a type-I topology (*18*, *20*−*22*), whereas novel isoenzymes (such as PKCδ and PKCϵ) exhibit a type-II topology, although the Ca^{2+}-binding site is degenerated (*19*, *23*).

In the C2 domains that bind Ca^{2+}, as in classical PKCs, the Ca^{2+}-binding site, which is formed mainly of five aspartate side chains, is located at the flexible top loops and binds two or three Ca^{2+} ions (*18*, *20*−*21*). The presence of phospholipid membranes increases the overall Ca^{2+} affinity and makes the Ca^{2+} binding highly cooperative (*15*, *28*−*31*). Anionic phospholipids have been shown to bind to the C2 domain of PKCα in two different locations, namely, the Ca^{2+}-binding pocket, where it interacts with one of the bound Ca^{2+} ions (*20*), and in the vicinity of the lysine-rich cluster located at strands β3 and β4 (*21*). It has been demonstrated both in vivo and in vitro that the C2 domain of PKCα mediates this Ca^{2+}-dependent binding (*8*−*9*).

In this paper, we will focus our attention on the classical PKCs (α, βI, βII, and γ). Although these proteins share similar structural and enzymatic properties, they are distributed in tissues and cells in a type-specific manner (reviewed in refs *32* and *33*), with different levels of expression. In this sense, PKCα is found in all cell types, while PKCβI and PKCβII are found in some tissues, and PKCγ is found only in the central nervous system (*34*). In addition, the level of specialization among classical PKCs is high. When all of these facts are taken into account, clarification of the differences in classical isoenzyme regulation is very interesting to explain their variable cellular localizations and levels of expression. We have chosen the C2 domains of these related isoenzymes to carry out a comparison of their thermal stability and their affinities for Ca^{2+} and phospholipid membranes because the C2 domain is heavily involved in regulating the activity of classical PKCs. The primary amino acid sequence of the C2 domains from different classical PKC isoenzymes is highly conserved (*35*−*37*), and furthermore, the 3D structures of the C2 domains from PKCα and PKCβI are also very similar (*18*, *20*−*22*); although no structural information is available for PKCγ, the high sequence identity indicates that this C2 domain might have a similar structure to that of the C2 domains from other classical PKCs.

Previous studies have already pointed to some differences among these three C2 domains in regards to their ligand-binding properties (*38*), as well as their secondary structure and susceptibility to thermal denaturation (*39*).

In the present paper, we have used calorimetric techniques to investigate the structural differences between the different classical PKCs isoenzymes. Isothermal titration calorimetry (ITC) and differential scanning calorimetry (DSC) are the only methods for the direct determination of the enthalpy changes (ΔH) (*40*). Using ITC experiments, the dissociation constant (K_d) and the stoichiometry (n) of the interaction between a protein and a ligand can also be obtained. On the other hand, DSC gives immediate access to the mechanism of protein denaturation and it can be used for protein−ligand interaction studies (*41*−*44*). The combination of both techniques provides a more comprehensive description of the thermodynamics of an interacting system. Some C2 domains from different proteins [phospholipase Cδ1−C2 domain (*45*), phospholipase A2c−C2 domain (*16*), phospholipase Dα and phospholipase Dβ−C2 domains (*46*), and PKCϵ−C2 domain (*47*)] and their interaction with ligands have also been studied using these methods.

EXPERIMENTAL PROCEDURES

Materials. 1-Palmitoyl-2-oleoyl-*sn*-glycero-3-phosphocholine (POPC) and 1-palmitoyl-2-oleoyl-*sn*-glycero-3-phospho-L-serine (POPS) were purchased from Avanti Polar Lipids, Inc. (Alabaster, AL). Ionophore A23187 and chelating resin (iminoacetic acid, Chelex-100) were purchased from Sigma (Madrid, Spain). Isopropyl-1-thio-β-D-galactopyranoside (IPTG) was purchased from Roche Diagnostics (Barcelona, Spain). Ni-NTA agarose was purchased from Quiagen (Hilden, Germany). Calcium-standard solution (Tritisol) was purchased from Merck (Barcelona, Spain). Water was distilled 2 times and deionized using a Millipore system from Millipore Ibérica (Madrid, Spain). All buffers and proteins were passed through a column with Chelex-100 to eliminate contaminant calcium. Residual calcium after Chelex-100 was measured using ICP-OE spectroscopy with a Perkin−Elmer Optima 2000 DV spectrometer (Perkin−Elmer, Wellesley, MA). The treatment with Chelex-100 eliminated almost all calcium from the buffers (residual calcium was less than 0.02 μM), but it could not remove all calcium from the protein solutions. Therefore, in this case, residual calcium was approximately a 4:1 molar ratio of protein/Ca^{2+}.

Preparation of Phospholipids. Lipid vesicles were generated by mixing chloroform solutions of POPC and POPS at the desired proportions (POPC/POPS, molar ratio of 2:3) and ionophore A23187 (at a 1000:1 molar ratio of phospholipid/ionophore). Lipids were dried from the organic solvent under a stream of oxygen-free nitrogen, and then the last traces of organic solvent were removed under vacuum for at least 2 h. Dried phospholipids were resuspended in the corresponding buffers by vigorous vortexing and then subjected to direct probe sonication (10 cycles of 15 s) to produce small unillamelar vesicles (SUVs).

Construction of the Expression Plasmids. PKCα and PKCβII cDNAs were kind gifts from Drs. Nishizuka and Ono (Kobe University, Kobe, Japan), while PKCγ cDNA was a kind gift from Dr. Tobias Meyer (Stanford University Medical School, Stanford, CA). The DNAs for the C2 domains of PKCα, PKCβII, and PKCγ were obtained as previously described (*39*, *48*).

Expression and Purification of the His-PKC−C2 Domains. The pET28c(+) plasmid containing PKC−C2 domains were transformed into BL21 (DE3) *Escherichia coli* cells. The bacterial cultures (OD_{600} = 0.6) were induced for 5 h at 30 °C with 0.5 mM IPTG. The cells were lysed by sonication in lysis buffer containing protease inhibitors (10 mM benzamidine, 1 mM PMSF, and 10 μg/mL trypsin inhibitor).

The lysis buffers for PKCα, PKCβII, and PKCγ C2 domains contained 25 mM Hepes at pH 7.4 and 100 mM NaCl, 20 mM MOPS at pH 6.8 and 100 mM NaCl, and 25 mM Tris-HCl at pH 8.0 and 100 mM NaCl, respectively. The soluble fraction of the lysate was incubated with Ni-NTA agarose for 2 h at 4 °C. The Ni beads were washed with lysis buffer containing 20 mM imidazole. The bound proteins were eluted with the appropriate lysis buffer containing 50, 250, and 500 mM imidazole. The six-histidine tag was removed after thrombin cleavage, and finally, the PKC−C2 domain was washed with the corresponding buffer and concentrated using an Ultrafree-5 centrifugal filter unit (Millipore Inc, Bedford, MA). Protein concentrations were determined by the BCA assay (*49*), using bovine serum albumin as the standard, and also by UV spectroscopy using the theoretical extinction coefficients of each protein in guanidium hydrochloride, with a very good agreement in the results of both methods. The purity of the samples was checked by a 15% SDS−polyacrylamide gel electrophoresis (*50*) and Coomassie Blue staining (Sigma, St. Louis, MO), revealing that it was higher than 95%. The native folding of the recombinant C2 domains produced in our laboratory has been widely confirmed by our previous X-ray crystallographic studies with the PKCα−C2 domain (*20*−*22*) and also using FTIR spectroscopy with the three C2 domains (*39*).

ITC. Binding of Ca^{2+} and lipids to the different C2 domains of classical PKC was studied by ITC using a Microcal MCS microcalorimeter (Microcal Inc., Northampton, MA). The instrument and its use have been described previously (*51*). Experiments were carried out at a constant temperature of 25 °C using a water bath. The buffers were 25 mM Hepes at pH 7.4 and 100 mM NaCl for PKCα−C2 domain, 20 mM MOPS at pH 6.8 and 100 mM NaCl for PKCβII−C2 domain, and 25 mM Tris-HCl at pH 8.0 and 100 mM NaCl for PKCγ−C2 domain. The reference cell contained Milli Q water. The concentration of each C2 domain in the reaction cell was 0.25 mM (approximately 4 mg/mL) in the case of the PKCα− and PKCγ−C2 domains and 0.2 mM (approximately 3.3 mg/mL) in the case of PKCβII−C2 domain. A 6 mM Ca^{2+} solution, prepared in the corresponding buffers of each protein using a concentrated calcium-standard solution, was loaded into the 280-μL syringe. This titration solution was injected with a stirring speed of 250 rpm at discrete intervals of 240 s in different ways for each sample. Ca^{2+} was added in 8-μL injections 36 times for the PKCα−C2 domain; 1-μL injection plus 20 μL 14 times for the PKCβII−C2 domain; and 1-μL injection plus 5 μL 10 times and 20 μL 11 times for the PKCγ−C2 domain. The C2 domains were titrated up to a Ca^{2+}/protein molar ratio of about 6, taking into account the volume of the reaction cell (approximately 1.4 mL) and the protein dilution effect produced by the injection of the titration solution into the cell.

SUVs (POPC/POPS, molar ratio of 2:3) were used to determine the binding of lipids to protein in the presence of saturating Ca^{2+}. The reaction cell contained the protein and a saturating concentration of Ca^{2+} (1 mM), as determined by the previous experiments. The lipid suspensions containing the same concentration of Ca^{2+} were added in serial injections of 1 μL (the first) and 15 μL (the rest). The concentration of proteins in the cell was about 0.2 mM (approximately 3.3 mg/mL), while the total concentration of lipids in the syringe was about 30 mM; therefore, the C2 domains were titrated up to a POPS/protein molar ratio of about 12, taking into account the POPS in the outer bilayer of the SUVs.

In both cases, the heat of dilution was measured by injecting the ligand into the corresponding buffer without the protein, and the value was then subtracted from the heat of reaction to obtain the effective heat of binding. The resulting titration data were analyzed and fitted to different models using the Origin for ITC software package supplied by Microcal to obtain the number of bound ligand molecules (n), the dissociation constants (K_d), and the enthalpy (ΔH) and the entropy (ΔS) changes of binding. The best-fitting of the experimental data was obtained using the *two-sets of sites model* for the binding of Ca^{2+} and the *one-set of sites model* for the binding of vesicles to the proteins in the presence of saturating calcium.

DSC. The theory of DSC and the thermodynamic interpretation of experiment data have been reviewed previously (*52*−*54*). Data collection and analysis were performed using Microcal MC-2 scanning microcalorimeter (Microcal Inc., Northamptom, MA) and Microcal Origin 5.0 (Microcal Software Inc., Northamptom, MA), respectively. The typical scan rates were 60 °C/h. A buffer−buffer baseline was subtracted from the sample scans, and then the concentration normalization was done. The denaturation heat capacity change (ΔC_p) was determined as the difference between the heat capacity of the native and the denatured forms of each protein sample extrapolated to the T_m (*40*). Finally, ΔH was determined after subtracting the baseline created connecting the signal below and above the transition using the cubic spline method.

The proteins were prepared in the corresponding buffers, and the final concentration was 0.15 mM (approximately 2.4 mg/mL). The buffers were 25 mM Hepes at pH 7.4, 100 mM NaCl, and 0.2 mM EGTA for the PKCα−C2 domain, 20 mM MOPS at pH 6.8, 100 mM NaCl, and 0.2 mM EGTA for the PKCβII−C2 domain, and 25 mM Tris-HCl at pH 8.0, 100 mM NaCl, and 0.2 mM EGTA for the PKCγ−C2 domain. The transitions of the C2 domains were also studied in the presence of different Ca^{2+} concentrations. The program designed by Fabiato (*55*) was used to calculate the total calcium concentration needed to give the desired available calcium concentrations, taking into account the composition of the buffer and the EGTA concentration.

To study the transition of the proteins in the presence of lipids, SUVs were mixed with the protein solutions. The lipid mixtures contained POPC/POPS (molar ratio of 2:3) and were prepared in the corresponding buffers, as described above, at a final concentration of 8 mM. Protein−lipid samples were also studied in the presence of different free Ca^{2+} concentrations.

RESULTS

ITC Studies. The thermodynamics of Ca^{2+} binding to the C2 domains from the three classical PKC isoenzymes at 25 °C were characterized by ITC experiments. In the case of the PKCα−C2 domain (Figure 1A), the binding data are consistent with one high-affinity site (with a K_d of 0.9 ± 0.3 μM) and two low-affinity sites (with a K_d of 22.2 ± 2.6 μM) (Table 1). It appears that Ca^{2+} binding to the first high-

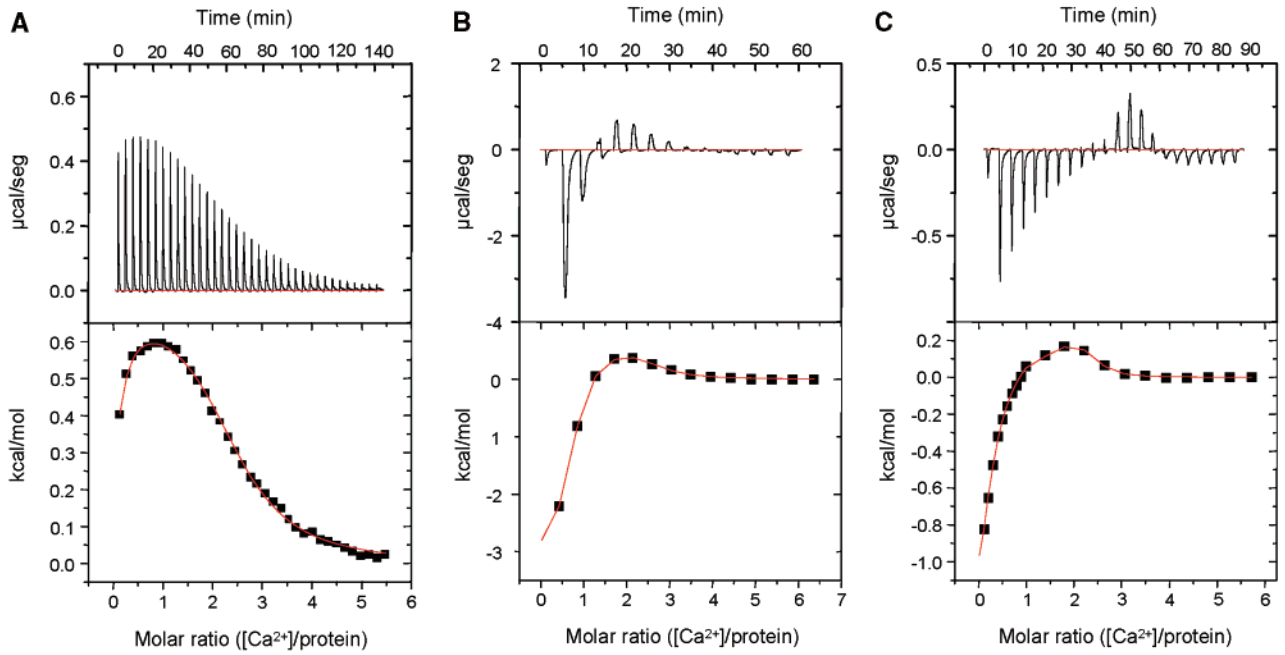

FIGURE 1: ITC data for calcium binding to the C2 domains of PKCα (A), PKC*β*II (B), and PKC*γ* (C) at 25 °C. The upper panels show the raw data for the titration of the protein with standard Ca^{2+}. The bottom panels show the integrated data obtained from the previous raw data, after subtracting the heat of dilution. The solid line in the bottom panels represents the best curve fit to the data, using the *two sets of sites model* from Microcal Origin. The thermodynamic parameters of this binding are shown in Table 1. The buffers and the different injections made for each protein are explained in detail in the text (see the Experimental Procedures).

Table 1: Thermodynamic Parameters of Ca^{2+} Binding to PKCα−, PKC*β*II−, and PC*γ*−C2 Domains at 25 °C[a]

protein	number of bound ligand molecules (n)	K_d (mM)	$\Delta H°$ (kcal/mol)	$\Delta S°$ (cal/mol^{-1} K^{-1})	$\Delta G°$ (kcal/mol)
PKCα−C2	$n_1 = 0.2 \pm 0.1$	0.9 ± 0.3	-2.3 ± 0.3	17.8 ± 0.3	-7.6 ± 0.2
	$n_2 = 2.3 \pm 0.2$	22.2 ± 2.6	0.74 ± 0.04	23.8 ± 0.2	-6.3 ± 0.1
PKC*β*II−C2	$n_1 = 0.6 \pm 0.1$	1.3 ± 0.2	-3.8 ± 0.3	14.3 ± 0.7	-8.0 ± 0.1
	$n_2 = 1.8 \pm 0.1$	17.2 ± 3.3	0.77 ± 0.08	24.4 ± 0.1	-6.5 ± 0.1
PKC*γ*−C2	$n_1 = 0.2 \pm 0.1$	0.8 ± 0.2	-3.6 ± 0.9	15.8 ± 2.0	-8.3 ± 0.2
	$n_2 = 2.1 \pm 0.1$	4.3 ± 1.3	0.29 ± 0.03	25.6 ± 0.6	-7.3 ± 0.2

[a] Mean and standard deviation values from the fitted data of three independent experiments are shown.

affinity site is exothermic with $\Delta H = -2.3 \pm 0.3$ kcal/mol, while the second set of sites binds Ca^{2+} endothermically with $\Delta H = +0.74 \pm 0.04$ kcal/mol. The number of Ca^{2+} ions bound per molecule of protein appears to be 0.2 ± 0.1 for the first site and 2.3 ± 0.2 for the second set of sites. These data suggest that the low-affinity site binds two Ca^{2+} ions and the high-affinity site, which presumably binds one Ca^{2+}, was partially filled at the beginning of the experiment, as seen through ICP-EO spectroscopy and commented in the *Materials* section of the Experimental Procedures. Although there is some evidence supporting the view that Ca^{2+} binding is cooperative (*38*), the analysis of the binding curve assuming independent sets of binding sites (*two sets of sites* model) yielded a better fit of the experimental data, which could partially be due to the initial saturation of the highest affinity site for Ca^{2+}.

Two different types of sites were also detected in the case of the PKC*β*II−C2 domain (Figure 1B), a high-affinity one (with a K_d of 1.3 ± 0.2 μM) and two low-affinity sites (with a K_d of 17.2 ± 3.3 μM). Again, the first high-affinity site is exothermic (with $\Delta H = -3.8 \pm 0.3$ kcal/mol), while the second low-affinity site is endothermic (with $\Delta H = +0.77 \pm 0.08$ kcal/mol). In this case, the number of Ca^{2+} ions bound per molecule of protein is 0.6 ± 0.1 for the first set of sites and 1.8 ± 0.1 for the second set (Table 1).

The same pattern was observed with the PKC*γ*−C2 domain (Figure 1C). The Ca^{2+} titration curve was consistent with a high-affinity site (K_d of 0.8 ± 0.2 μM), which binds one Ca^{2+} molecule ($n = 0.2 \pm 0.1$) exothermically ($\Delta H = -3.6 \pm 0.9$ kcal/mol), and two low-affinity sites (K_d of 4.3 ± 1.3 μM), which bind two Ca^{2+} ions ($n = 2.1 \pm 0.1$) endothermically ($\Delta H = +0.29 \pm 0.03$ kcal/mol) (Table 1).

In all cases, the Ca^{2+} binding to the highest affinity set of sites is aided by both entropic and enthalpic contributions, whereas the Ca^{2+} binding to the second and low-affinity set of sites is entropically driven (Table 1).

The experiments were performed at 25 °C, which is the usual temperature for ITC measurements and is low enough from the beginning of the thermal denaturation of the proteins. Furthermore, similar binding experiments were performed at 37 °C, and the results were practically identical (data not shown).

The binding of phospholipids to the three domains was also studied in the presence of saturating Ca^{2+} (1 mM, giving a Ca^{2+}/protein molar ratio of 5:1). SUVs composed of POPC/POPS (molar ratio of 2:3) were used as the ligand. Because

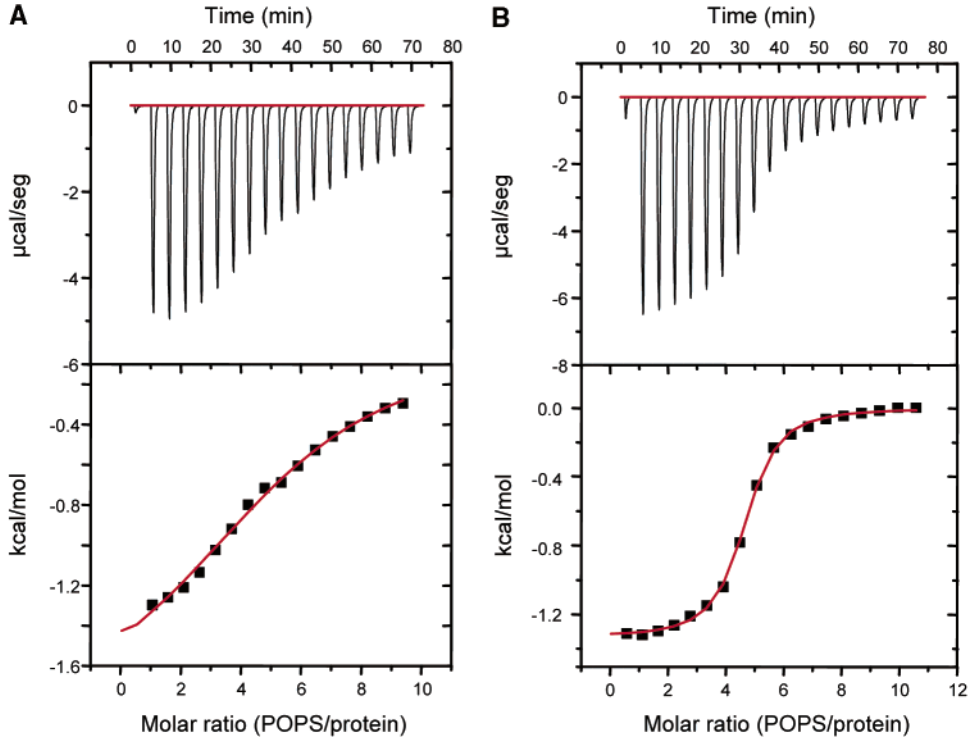

FIGURE 2: ITC data for binding of POPC/POPS (molar ratio of 2:3) SUVs to the C2 domains of PKCα at 25 °C, in the absence of Ca^{2+} (A) and in the presence of saturating Ca^{2+} (B). The upper panels show the raw data for the titration of 0.2 mM protein (approximately 3.3 mg/mL) with 30 mM lipid vesicles. The bottom panels show the integrated data obtained from the previous raw data, after subtracting the dilution experiments. The solid line in the bottom panels represents the best curve fit to the experimental data, using the *one set of sites model* from Microcal Origin. Similar data were obtained for the PKCβII− and PKCγ−C2 domains (data not shown). The thermodynamic parameters of this binding are shown in Table 2. The buffers and the different injections made for each protein are explained in detail in the text (see the Experimental Procedures).

Table 2: Thermodynamic Parameters of POPC/POPS (molar ratio of 2:3) SUVs Binding to PKCα−, PKCβII−, and PKCγ−C2 Domains in the Presence of Saturating Ca^{2+} at 25 °C[a]

protein	number of bound ligand molecules (n)	K_d (mM)	$\Delta H°$ (kcal/mol)	$\Delta S°$ (cal/mol^{-1} K^{-1})	$\Delta G°$ (kcal/mol)
PKCα−C2	4.5 ± 0.1	18.0 ± 1.2	−1.33 ± 0.01	17.3 ± 0.1	−6.5 ± 0.1
PKCβII−C2	5.6 ± 0.1	9.7 ± 1.5	−0.50 ± 0.01	21.3 ± 0.3	−6.8 ± 0.1
PKCγ−C2	4.9 ± 0.1	18.4 ± 2.3	−1.30 ± 0.02	17.3 ± 0.2	−6.5 ± 0.1

[a] Mean and standard deviation values from the fitted data of three independent experiments are shown.

C2 domains bind to anionic phospholipid, the total lipid concentration was normalized considering the proportion of POPS in the mixture and also the fact that only the outer surface of the lipid bilayer vesicle (about 60% of total lipid) was accessible to the protein. In the absence of Ca^{2+} (Figure 2A), only a weak interaction was observed (K_d = 430 ± 23 μM) and it was not possible to reach saturation. The results were clearly different in the presence of saturating Ca^{2+} but similar for the three C2 domains (Figure 2B), all showing exothermic binding with $\Delta H = -1.33 \pm 0.01$ kcal/mol for PKCα−C2, $\Delta H = -0.50 \pm 0.01$ kcal/mol for PKCβII−C2, and $\Delta H = -1.30 \pm 0.02$ kcal/mol for PKCγ−C2 (Table 2). Lipids were bound with similar affinity, showing a K_d of 18.0 ± 1.2 μM for PKCα−C2, 9.7 ± 1.5 μM for PKCβII−C2, and 18.4 ± 2.3 μM for PKCγ−C2 (Table 2). Although the number of phospholipid molecules bound to protein is difficult to assess in this case because of the nature of the ligand (i.e., phospholipid vesicles), the results were very similar in all cases: 4.5 ± 0.1 POPS molecules for the PKCα−C2 domain, 5.6 ± 0.1 for the PKCβII−C2 domain, and 4.9 ± 0.1 for the PKCγ−C2 domain (Table 2). POPS binding to the C2 domain is stabilized by both entropic and enthalpic contributions, although the former is the main driving force in all cases (Table 2).

The increase in lipid affinity of the three C2 domains in the presence of Ca^{2+} suggests that the weak interaction with lipid vesicles detected in the absence of the ion (Figure 2A) might reflect that an unspecific binding was taking place.

DSC Studies. To gain further insight into the structural differences between the three C2 domains belonging to the classical PKC isoenzymes, as studied here, we have compared their unfolding behavior upon thermal denaturation, at the same time characterizing the effect of incorporating different ligands, such as Ca^{2+} and anionic phospholipids (POPS).

The thermodynamic parameters obtained from the DSC transitions of the classical PKCs C2 domains in the absence of ligands, i.e., in the presence of 0.2 mM EGTA, are presented in Table 3.

The unfolding of the PKCα−C2 domain was greatly affected by the concentration of Ca^{2+} (Figure 3A). Whereas, in the absence of Ca^{2+}, the onset of the transition takes place

Table 3: Thermodynamic Data of the Thermal Denaturation of the Classical PKCs C2 Domains in the Absence of Ligands, i.e., in the Presence of 0.2 mM EGTA, Obtained from the Fitted DSC Curves[a]

protein	T_m (°C)	$T_{1/2}$ (°C)	ΔC_p (kcal/mol^{-1} K^{-1})	$C_{p,max}$ (kcal/mol^{-1} K^{-1})	ΔH (kcal/mol)	ΔH_{vH} (kcal/mol)
PKCα−C2	49.7 ± 0.2	5.8 ± 0.1	1.09 ± 0.07	2.99 ± 0.24	27.9 ± 2.0	110.7 ± 4.6
PKCβ II−C2	46.7 ± 0.2	5.1 ± 0.1	0.49 ± 0.04	3.85 ± 0.29	33.1 ± 2.6	119.7 ± 6.2
PKCγ−C2	47.8 ± 0.2	5.0 ± 0.1	0.59 ± 0.04	3.56 ± 0.28	34.2 ± 2.1	115.9 ± 3.9

[a] Mean and standard deviation values from the fitted data of three independent experiments are shown.

at 40.2 °C (with a T_m at 49.8 °C), the progressive addition of Ca^{2+} gradually shifts the transition peak toward higher temperatures, so that, at a protein/Ca^{2+} molar ratio of 1:1000, the transition started at 74.2 °C and the T_m was 80.3 °C. This means that the protein structure is strongly stabilized by Ca^{2+} binding.

A study of the thermal stability of the PKCβII−C2 domain (Figure 3B) showed a qualitatively similar behavior. In the absence of Ca^{2+}, the T_m was 46.7 °C, which is slightly lower than that of the PKCα−C2 domain, although the onset of the thermal transition was also around 40 °C. Again, the addition of increasing Ca^{2+} concentrations shifted the transitions toward higher temperatures, with the protein structure being stabilized as before. At the highest Ca^{2+} concentration studied (protein/Ca^{2+} molar ratio of 1:1000), the onset temperature of the transition was 74.4 °C and the T_m was 78.8 °C.

The PKCγ−C2 domain also showed a gradual increase in the transition temperature (Figure 3C) upon the addition of increasing Ca^{2+} concentrations. Thus, the T_m values of this isoenzyme shifted from 47.8 °C in the absence of Ca^{2+} (i.e., in the presence of 0.2 mM EGTA) to 85.4 °C at a protein/Ca^{2+} molar ratio of 1:1000.

In all cases, the width of the transitions was greater at protein/Ca^{2+} molar ratios lower than 1:50, which may reflect the existence of an heterogeneous protein population composed of molecules with a different content of bound Ca^{2+} within the transition interval. Further increases in Ca^{2+} concentration gave rise to narrower transition peaks, probably because of a protein state in which all of the binding sites were completely saturated with Ca^{2+} and, as expected for a system in which denaturation proceeds with simultaneous dissociation of bound ligand, the shift in the T_m with increasing [Ca^{2+}] is a nonsaturable effect.

The addition of POPC/POPS (molar ratio of 2:3) SUVs to give a protein/phospholipid molar ratio of 1:50 greatly modified the profiles of the thermal transitions, so that in the absence of Ca^{2+} the transition peak of the PKCα−C2 domain was considerably widened and also slightly shifted toward lower temperatures in the presence of the lipid vesicles (Figure 4A). The width at half-height of this transition increased from 5.8 to 20.5 °C upon the addition of lipid vesicles. The broadening of the peak suggested the coexistence of protein populations with a differing content of bound lipids within the transition interval. It is quite interesting that the addition of increasing concentrations of Ca^{2+} progressively sharpened the thermal transitions, which became similar in shape to those found in the absence of lipids at a protein/Ca^{2+} molar ratio of 1:10. This probably reflects the enhancement of lipid binding mediated by Ca^{2+} observed by the direct titration using ITC (Figure 2). The small fall in the T_m of the transition in the presence of lipid vesicles without Ca^{2+} (49.8 °C in the absence of both Ca^{2+} and lipids and 48.5 °C in the absence of Ca^{2+} but in the presence of lipid vesicles) might either reflect slight protein destabilization or the fact that the denatured protein form shows a higher affinity for the lipid.

The addition of POPC/POPS (molar ratio of 2:3) SUVs to the PKCβII−C2 domain at the same protein/lipid molar ratio also induced a broadening and a small shift toward lower transition temperatures. The temperature onset was located at 36.8 °C, and the T_m was 43.5 °C (temperature onset at 40 °C and T_m at 46.7 °C, in the absence of both ligands) (Figure 4B). A progressive reduction in the peak width was observed as the Ca^{2+} concentration increased, and the shape of the transitions became similar to those found in the absence of lipids, again at a (protein/[Ca^{2+}]) molar ratio of 1:10. Anyway, the initial broadening of the PKCβII−C2 domain transition was smaller than that observed for the PKCα−C2 domain (the width at half-height increased from 5.1 °C in the absence of phospholipids to 8.9 °C in the presence of lipid vesicles).

Similar effects were observed upon addition of phospholipid vesicles to the PKCγ−C2 domain in the absence of Ca^{2+} at the same protein/lipid molar ratio (Figure 4C). Thus, the $T_{1/2}$ was 5.0 °C in the absence of vesicles and 7.9 °C in the presence of phospholipids. This increase in the transition width was not so big as that of the PKCα−C2 domain, probably because the PKCγ−C2 domain had a higher binding affinity and in this case most protein was bound to the vesicles. Besides, the shift of the peak to lower temperatures was also smaller than in the other two domains (T_m at 47.8 °C in the absence of both ligands and at 46.7 °C in the absence of Ca^{2+} but in the presence of lipid vesicles).

Figure 5 shows the dependence of the transition temperature on the Ca^{2+} concentration both in the absence and in the presence of lipid vesicles. The increase in the T_m was slightly different for each C2 domain, and at a given Ca^{2+} concentration, the increase of the T_m in the presence of lipid vesicles (Figure 5B) was higher than in its absence (Figure 5A), reflecting the cooperative effect of both ligands on the stabilization of the protein structure, in agreement with previous results (*39*, *48*).

The denaturation of the PKC−C2 domains studied here was irreversible both in the absence and in the presence of ligands. To gain further information about the system behavior, the same protein samples were scanned at different rates, i.e., 15, 30, and 60 °C/h, both in the absence (Figure 6A) and in the presence (Figure 6B) of Ca^{2+}. The simplest model that can reflect such behavior would be

$$N + mL \leftrightarrow NL_m \leftrightarrow U + mL \quad (1)$$
$$\downarrow$$
$$F$$

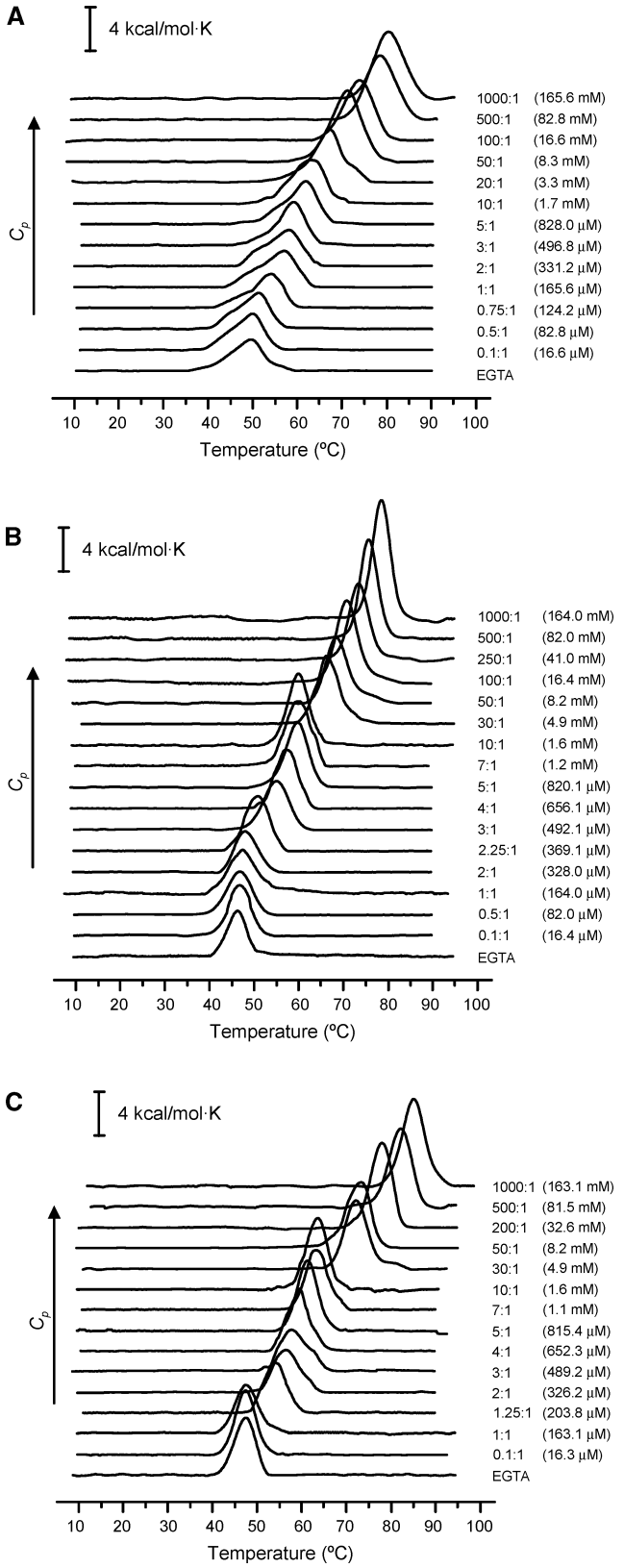

FIGURE 3: DSC scans of the C2 domains of PKCα (A), PKCβII (B), and PKCγ (C) in the presence of different Ca^{2+} concentrations. The protein concentration was 0.15 mM (approximately 2.4 mg/mL) and the scanning rate was 60 °C/h. The Ca^{2+} concentration is shown as the total Ca^{2+} concentration available for the protein, taking into account the composition of the buffers, especially the EGTA content. These values are expressed in a molar concentration and in a Ca^{2+}/protein molar ratio. The DSC scans were analyzed using the Microcal Origin software (see the Experimental Procedures).

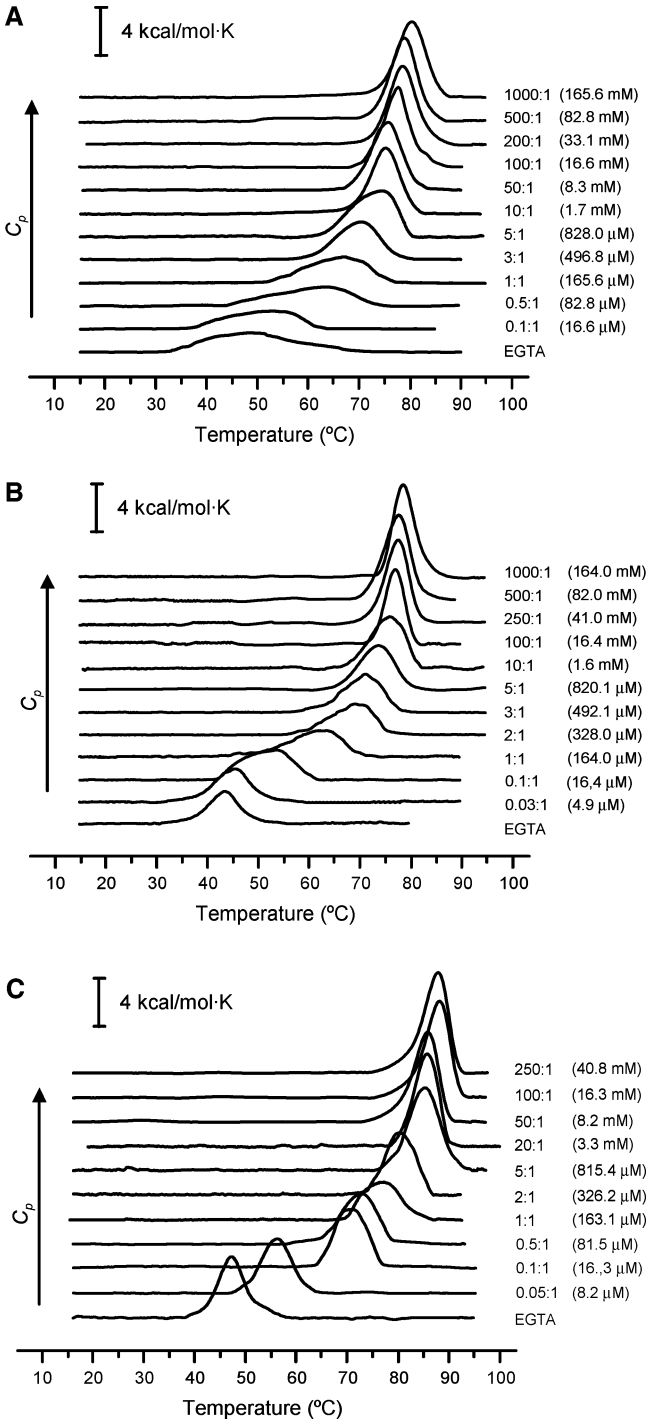

FIGURE 4: DSC scans of the C2 domains of PKCα (A), PKCβII (B), and PKCγ (C) in the presence of 8 mM POPC/POPS (molar ratio of 2:3) SUVs with different Ca^{2+} concentrations. The protein concentration was 0.15 mM (approximately 2.4 mg/mL), and the scanning rate was 60 °C/h. The Ca^{2+} concentration is shown as the total Ca^{2+} concentration available for the protein, taking into account the composition of the buffers, especially the EGTA content. These values are expressed in a molar concentration and in a Ca^{2+}/protein molar ratio. The DSC scans were analyzed using the Microcal Origin software (see the Experimental Procedures).

where N is the native protein form, L is the ligand, NL_m is the ligand bound protein form, U is the unfolded protein, and F is the irreversibly denatured final state. In systems where denaturation occurs as a kinetically controlled process, the transitions depend on the scanning rate (*56*, *57*), but in our case, the DSC scans at different rates of heating were

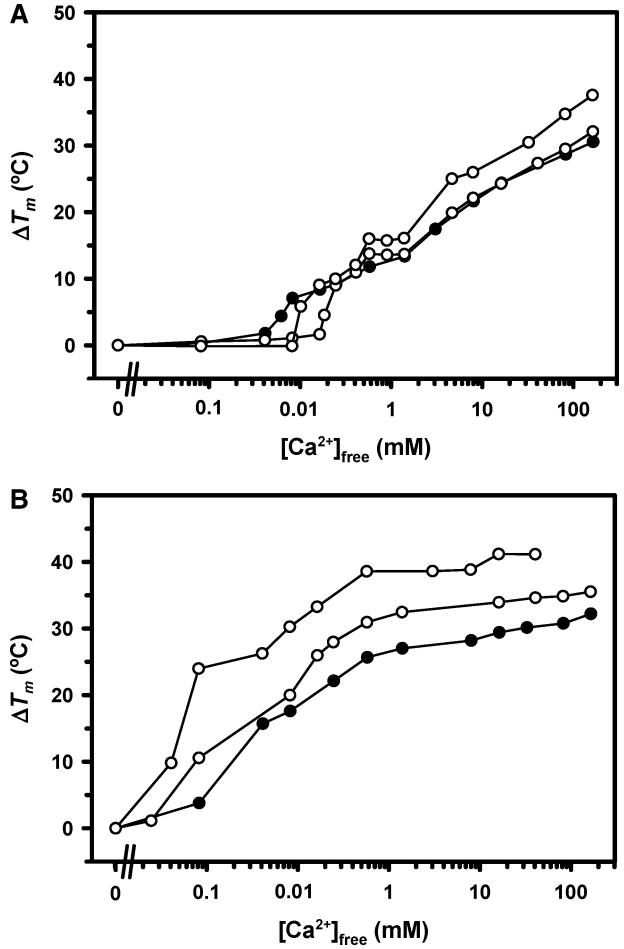

FIGURE 5: Effect of Ca^{2+} concentration on the T_m of the PKCα−C2 domain (black circles), PKCβII−C2 domain (white circles), and PKCγ−C2 domain (gray circles), in the absence (A) or in the presence (B) of POPC/POPS (molar ratio of 2:3) SUVs. The increase of T_m (ΔT_m) was calculated as the difference between the T_m at each Ca^{2+} concentration and the T_m in the absence of this ligand. Ca^{2+} concentration was expressed as the Ca^{2+}-free concentration at the T_m (see ref *59*).

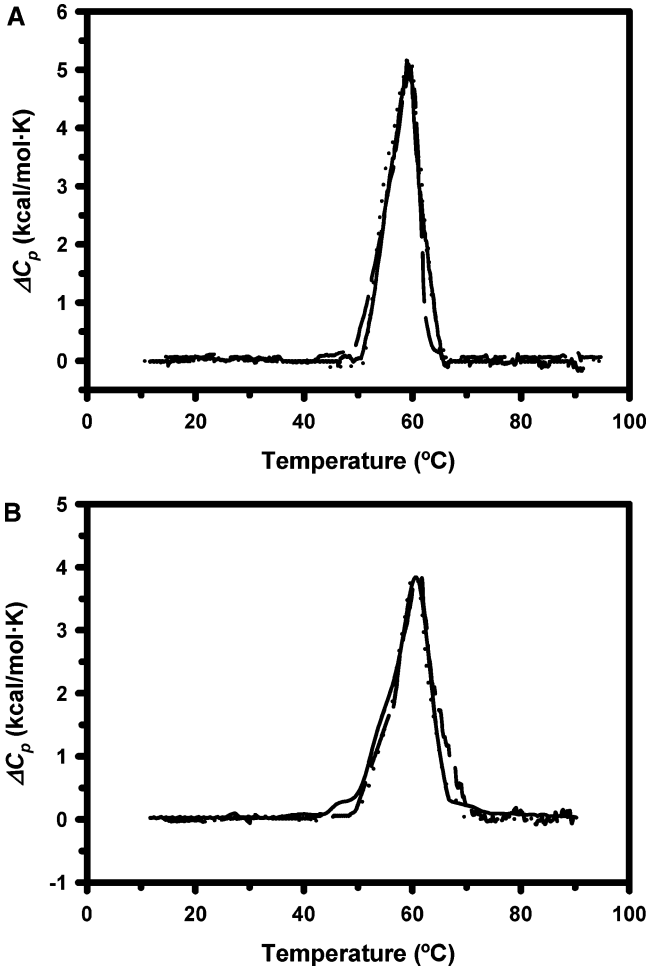

FIGURE 6: Effect of the scanning rate on the excess heat capacity of the PKCα−C2 domain in the absence of ligands (A) and in the presence of 5:1 (Ca^{2+}/protein) molar ratio (B). The protein concentration (0.15 mM, approximately 2.4 mg/mL) and buffer composition were the same in all cases. The scan rates were 60 °C/h (—), 30 °C/h (- - -), and 15 °C/h (•••). Similar results were obtained with the C2 domains of PKCβII and PKCγ (data not shown).

very similar (Figure 6). The easiest explanation for this behavior is assuming that the irreversible step proceeds at significant rates only at temperatures above the T_m and that the calorimetric traces would differ little from those corresponding to the reversible unfolding model (*56*, *57*). Accordingly, denaturation of the PKC−C2 domains can be analyzed in terms of equilibrium thermodynamics without large errors (*56*, *57*).

For a system in equilibrium, in which the protein undergoes denaturation with simultaneous dissociation of bound ligands, under saturating conditions, the dependence of the T_m on the ligand concentration can be approximated by the following van't Hoff integrated equation, as previously described (*58*):

$$\ln[L] = -\frac{\Delta H_{vH}}{nR}\frac{1}{T_m} + \text{constant} \qquad (2)$$

where ΔH_{vH} is the van't Hoff enthalpy, L the free ligand concentration, n the number of bound ligands, and T_m is the transition maximum temperature at this ligand concentration. The free cation concentration at the T_m can be estimated as $[Ca^{2+}]_{free} = [Ca^{2+}]_{total} - [\text{protein-binding sites}]/2$ (*59*), and the results are shown in Figure 7. The slope of the linear plots provides an estimation of the number of binding sites involved in the structural stabilization of the PKC−C2 domains, using the ΔH_{vH} values reported in Table 3. In the absence of lipid vesicles, n was close to 2 (i.e., 1.72 ± 0.02 for the PKCα−C2 domain, 1.99 ± 0.05 for the PKCβII−C2 domain, and 2.13 ± 0.03 for the PKCγ−C2 domain), although the number of Ca^{2+}-binding sites might be 3, as detected by ITC.

For a system with two sets of independent sites and considering, as in eq 2, that the denaturation enthalpy change is constant in the transition interval, the above van't Hoff integrated equation depicting the dependence of the T_m on the ligand concentration can be expressed as (*60*)

$$\ln[(1 + K_L^1[L])^{n_1}(1 + K_L^2[L])^{n_2}] = -\frac{\Delta H_{vH}^0}{nR}\left(\frac{1}{T_m} - \frac{1}{T_m^0}\right) \qquad (3)$$

where K_L^i and n_i are respectively the binding constant and the number of sites for set i and ΔH_{vH}^0 and T_m^0 are the van't Hoff enthalpy and the transition temperature in the absence

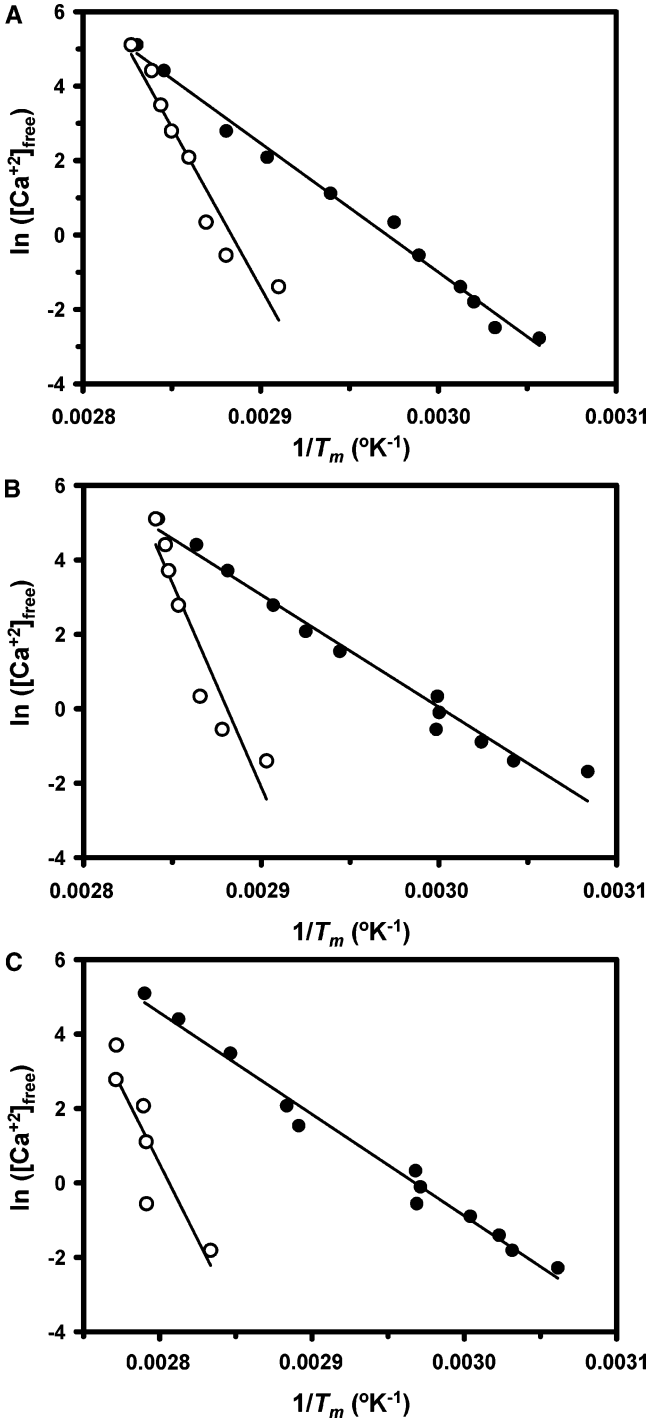

FIGURE 7: Integrated van't Hoff plots of the effect of increasing Ca^{2+} concentration on the thermal denaturation of the PKCα−C2 domain (A), PKCβII−C2 domain (B), and PKCγ−C2 domain (C), in the absence (●) or in the presence (○) of POPC/POPS (molar ratio of 2:3) SUVs. The straight lines show the best linear fit to the data.

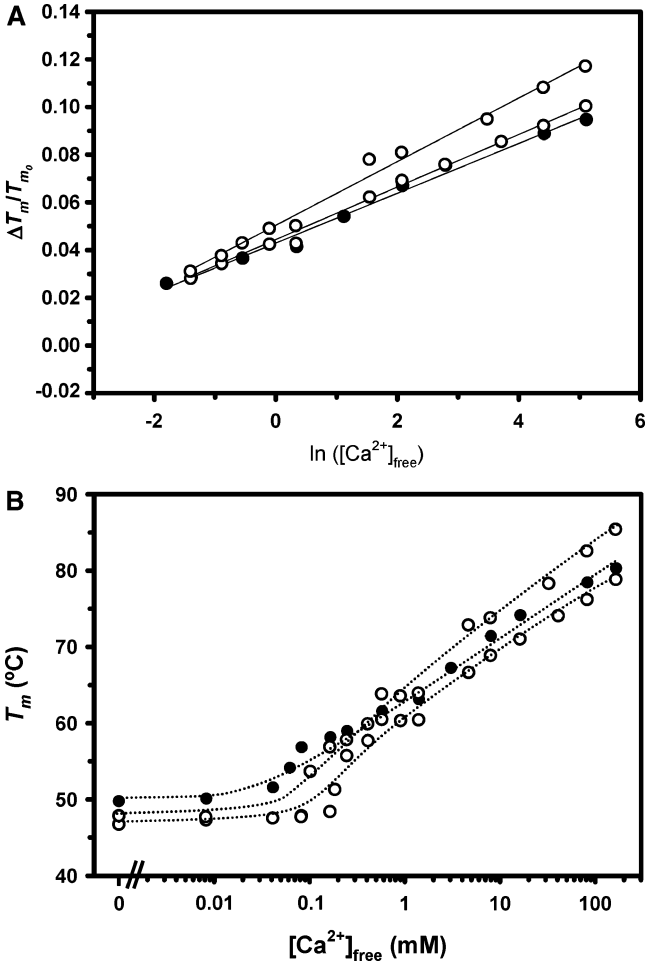

FIGURE 8: (A) Effect of increasing Ca^{2+} concentration on the change of the normalized midpoint transition temperature of the PKCα−C2 domain (black circles), PKCβII−C2 domain (white circles), and PKCγ−C2 domain (gray circles). The straight lines show the best linear fit to the data. (B) Effect of increasing Ca^{2+} concentration on T_m of the PKCα−C2 domain (black circles), PKCβII−C2 domain (white circles), and PKCγ−C2 domain (gray circles). The dotted lines show the best nonlinear fit to the data, using the values of the binding constants for each C2 domain obtained from the thermodynamic treatment of the DSC data (see the text). The nonlinear fit was made with the Microcal Origin software.

of ligands. At saturating Ca^{2+} concentrations ($1 + K_L^i[L] \gg 1$), this expression can easily be transformed into

$$\frac{\Delta T_m}{T_m^0} = \frac{RT_m^0}{\Delta H_{vH}^0} \ln(n_1 K_L^1 + n_2 K_L^2) - (n_1 + n_2) \frac{RT_m^0}{\Delta H_{vH}^0} \ln[L] \quad (4)$$

where $\Delta T_m = T_m - T_m^0$. Using this equation and plotting ($\Delta T_m/T_m^0$) vs ln([Ca^{2+}]), we obtain an estimation of the number of sites ($n_1 + n_2$) and the apparent binding constants of the ligands involved in the process. As expected from Figure 7, in the absence of lipid vesicles (Figure 8A), the values of n derived from the slopes of the plots were again near 2 (1.77 ± 0.02 in the case of the PKCα−C2 domain, 1.96 ± 0.04 in the case of the PKCβII−C2 domain, and 2.15 ± 0.03 in the case of the PKCγ−C2 domain). The y-axis intercepts yielded average binding constants which, when expressed as dissociation constants, were very similar to the K_d of the second set of sites extrapolated to temperatures around the T_m, using the dissociation constant and the enthalpy changes measured by ITC at 25 °C (Table 1). These results suggest that the stabilization observed by DSC mainly reflects the saturation of the low-affinity Ca^{2+}-binding sites.

Figure 8B shows a nonlinear fit of the T_m versus [Ca^{2+}]$_{free}$, in terms of eq 4, assuming $n = 2$, and using the ligand concentration, [L], and the K_L values at the T_m (calculated by the van't Hoff equation, with the data reported for the low-affinity set of sites in Table 1) as independent variables

and T_m^0 and ΔH_{vH}^0 as the fitting parameters. The analysis was performed using the Microcal Origin software, and the best fitting values derived for T_m^0 and ΔH_{vH}^0 were in very good agreement with the data directly calculated from the DSC traces (50.9 ± 0.5 °C and 140 ± 5 kcal/mol for the PKCα−C2 domain, 47.5 ± 0.8 °C and 151 ± 8 kcal/mol for the PKCβII−C2 domain, and 48.1 ± 0.6 °C and 131 ± 6 kcal/mol for the PKCγ−C2 domain). These results strongly suggest that the observed stabilization of the three PKC−C2 domains can be mainly accounted for by Ca^{2+} binding to the low-affinity set of sites.

As commented above, the addition of lipid vesicles widened the peak transitions, suggesting the coexistence of protein populations with different contents of bound lipids within the transition interval. Besides, the addition of increasing concentrations of Ca^{2+} progressively sharpened the thermal transitions, reflecting the enhancement of lipid binding. The complexity of the system in these conditions makes it difficult to perform such a reliable thermodynamic analysis as above. Nevertheless, the observed shift of the ΔT_m versus [Ca^{2+}] concentrations toward lower ligand concentrations upon the addition of phospholipid vesicles (Figure 5) suggests an increase in the affinity of Ca^{2+} toward its second set of sites.

DISCUSSION

Although the sequence and the general structure of the C2 domains of the classical PKCs are very similar (*35*−*37*), the Ca^{2+} and phospholipid affinities and also the behavior during the thermal denaturation in the presence of both ligands are different. In principle, these subtle differences among the classical C2 domains may be significant in physiological conditions when explaining their selective regulation and their distinct functional specializations. The different classical PKC isoenzymes are distributed in tissues and cells in a type-specific manner, with different levels of expression (for reviews, see refs *32* and *33*). Hence, whereas PKCα and PKCβ are widely expressed in various tissues and cells, PKCγ is found only in the central nervous system (*1*, *2*). These isoenzymes also have highly specialized functions, as seen in relation to cancer, for example. Abnormal levels of these isoenzymes have been found in many transformed cell lines and in several human tumors (*61*). In this sense, high levels of PKCα lead to a more aggressive tumor phenotype (*62*), and it has been reported that this isoenzyme is involved in the suppression of apoptosis (*63*). PKCβI overexpression leads to tumor formation in R6 rat fibroblasts (*64*), while PKCβII can be used as a marker of colon cancer (*65*) and is involved in some diabetic problems (*66*, *67*). Finally, PKCγ is involved in the development of injury-induced persistent pain (*68*, *69*) and tumor formation in epithelial cells in vivo (*70*).

Although the global Ca^{2+} binding to the C2 domains of classical PKC isoenzymes is similar as seen through ITC, some differences can be observed among these proteins, especially in the binding of Ca^{2+} to the low-affinity set of sites, with the PKCγ−C2 domain showing the highest affinity. These binding results also differ from data obtained using C2 domains from other proteins previously reported. In this sense, several C2 domains from different proteins have been studied using ITC and they all showed variations in both the number of sites for Ca^{2+} and the nature of the binding driving forces. For example, the C2 domains from the phospholipases A2c (*16*), Cδ1 (*45*), and Dα (*46*) showed just one set of sites that bind Ca^{2+} in an exothermic way. In contrast, when the C2 domain of fragmin 60 was analyzed, Ca^{2+} was bound exothermically to two sets of binding sites (*71*). Moreover, the C2 domain of the phospholipase Dβ showed two sets of Ca^{2+}-binding sites (*46*); the first bound just one Ca^{2+} ion endothermically, while the second set of sites bound two Ca^{2+} ions exothermically.

In our case, the global Ca^{2+} stoichiometry (i.e., three Ca^{2+} ions) agrees with the recent high-resolution structural results obtained using X-ray diffraction with the PKCα−C2 (*21*) and PKCβI−C2 (*18*) domains.

It is worth noting that a previous study based on fluorescence spectroscopy (*38*) concluded that C2 domains from PKCβ and PKCγ isoenzymes bind three Ca^{2+} ions, while the PKCα−C2 domain only binds two, and that only the PKCβ−C2 domain shows cooperativity. Our present work cannot provide information about the cooperativity of the process because of the mathematical model used for the fitting of the data (*two set of sites* model). The Ca^{2+} stoichiometry for the C2 domains of PKCβ and PKCγ obtained with this ITC study is in perfect agreement with the previous fluorescence work (*38*) but differs in the case of the PKCα−C2 domain. This different stoichiometry for the PKCα−C2 domain would probably be due to the different experimental conditions employed. Nevertheless, it is possible that the third Ca^{2+} ion in the PKCα−C2 domain, detected here by ITC and in a previous X-ray diffraction study (*21*), either binds weakly to the domain or even dissociates too rapidly to be detected using the stopped-flow analysis described in the fluorescence spectroscopic study (*38*). It is difficult to assess which of the experimental conditions are more physiologically relevant because lipid and protein microdomains are known to be involved in these signaling pathways. The calculation of their real effective concentrations in the cell is an arduous task.

The presence of Ca^{2+} substantially enhances the interaction between these C2 domains and phospholipid membranes, a fact that reflects the important role played by Ca^{2+} as a bridge between the protein and the anionic phospholipids in the membrane (*20*, *21*). In the presence of a saturating Ca^{2+} concentration, the affinity of the three C2 domains for anionic phospholipids was similar, although it was slightly higher in the case of the PKCβII−C2 domain. This higher affinity is due to the entropic change and probably reflects either a bigger desolvation in the phospholipid-binding surface or a lower immobilization of the region involved in the interaction with the anionic phospholipid. It is obvious that the conditions with the greatest physiological implications are those involving phospholipid vesicles and subsaturating concentrations of Ca^{2+}. Unfortunately, no clear conclusions could be obtained in these conditions, because the binding of both Ca^{2+} and anionic phospholipids are enhanced simultaneously and the data could not be quantitatively analyzed.

It is difficult to assess the exact meaning of the number of phospholipids bound per protein molecule because phospholipid vesicles (and not individual molecules in solution) were used. It is clear that the data given in Table 2 are an overestimation with respect to the number of phospholipid molecules that are really bound. Nevertheless, it is interesting

that the calculated ratios seem to be compatible with those previously deduced from X-ray crystallographic studies (*21*), where the PKCα−C2 domain was concluded to be able to interact at the Ca^{2+}-binding site with one anionic phospholipid plus a phosphate group, which might indicate that a second phospholipid enters here in vivo, while another phospholipid enters in the lysine-rich cluster.

In our case, the use of DSC revealed that the interaction between these three C2 domains and ligands was rather complex. The binding of Ca^{2+} to the C2 domains of classical PKCs protects them from thermal denaturation, as shown by the shift of the T_m toward higher temperatures. Besides, this nonsaturable increase in the T_m with the Ca^{2+} concentration seems to be primarily mediated by the interaction of Ca^{2+} with its low-affinity sites. The enthalpic stabilization of the domain structure promoted by increasing concentrations of Ca^{2+} can be accounted for by the heat capacity increase of the proteins upon thermal denaturation (*60*).

Although ITC and DSC are methods for the determination of the different thermodynamic parameters of an interaction process, the information revealed by each one is not exactly the same. It is possible that a certain ligand concentration might not show a clear change in protein stability (as seen through DSC), although the ligand is bound (as detected by ITC). In some cases, the ligand binding does not produce stabilization of the structure, and even it can destabilize the protein (*72*).

At the same protein/Ca^{2+} molar ratios, the protein denaturation significantly increases the concentration of free ligand as the transition takes place. In this case, asymmetric DSC transition traces can be obtained (*60*), as observed in our case (Fugures 3 and 4). These asymmetric DSC traces are due either to the denaturation of the protein forms with less ligand bound or to the progressive stabilization of the protein native state during the transition, caused by the decrease of the apparent denaturation constant at a determined temperature when the concentration of free ligand increases (*60*, *73*).

The addition of anionic phospholipids in the absence of Ca^{2+} gave place to broad transitions, which gradually became narrower as the Ca^{2+} concentration increased. These wide transitions could be related with the interaction of the phospholipid with the lysine-rich cluster of the C2 domains, where Ca^{2+} is not involved (*21*), and might reflect the presence of a heterogeneous protein population with different phospholipid-bound states. There was also a slight shift in the T_m toward lower temperatures, which might reflect protein destabilization in the absence of Ca^{2+} or a higher affinity of the denatured protein for the lipid (*74*, *75*). Although the favorable protein−ligand interactions typically stabilize the protein structure, some studies have revealed certain kinds of destabilization mediated by ligand binding (*72*). It is possible that the lipid interactions with the lysine-rich cluster reduce the transition cooperativity, probably through the β-sandwich core of the C2-domain structure, or that the lipid establishes some detergent-type interactions with the protein in these conditions.

The protective effect of the ligand binding (Ca^{2+} alone or both Ca^{2+} and anionic phospholipids) against thermal denaturation was slightly different for the three C2 domains, particularly in the presence of phospholipids. In the case of the PKCα−C2 domain, this protective effect was more gradual than in the case of the PKCβII− or PKCγ−C2 domains, where the increase of the T_m was more abrupt. In this sense, the binding of approximately the same number of Ca^{2+} ions, as seen through ITC, has a different physiological significance for each C2 domain. In other words, at the same Ca^{2+} concentration, i.e., approximately the same Ca^{2+}-saturating state, the protective effect is different for each C2 domain. As shown above, the stabilization detected by DSC with increasing Ca^{2+} concentrations seems to be mainly mediated by saturation of the low-affinity binding sites. The high-affinity set of sites does not have a strong effect on the increase in the T_m, perhaps because of the very slow release of Ca^{2+} from this kind of site during denaturation.

Current denaturation results agree very well with a previous study based on infrared spectroscopy (*39*), where it was concluded that denaturation temperatures for the three C2 domains were very similar to those reported here, both in the absence and in the presence of ligands. Furthermore, the PKCβII−C2 was sightly less stable in the absence of Ca^{2+}, whereas the PKCα−C2 domain was the most stable one, both in the presence of Ca^{2+} and in the presence of both Ca^{2+} and phospholipids.

Interestingly, the three C2 domains studied here undergo a strong structural stabilization against thermal denaturation when interacting with Ca^{2+}. Ligand-induced conformational changes have not been checked through X-ray diffraction because protein crystallyzation devoid of Ca^{2+} has failed so far. However, recent results obtained using FTIR (*39*) indicated that Ca^{2+} induces only subtle changes in the secondary structure of these three C2 domains, although Ca^{2+} binding significantly increased the differences in thermal stability among them. The different sensitivities to thermal denaturation observed here by DSC and previously by FTIR (*39*) likely arise from different backbone motions and would, hence, probably be related with changes in dynamics rather than with significant structural changes. This type of information cannot be provided by high-resolution structural studies.

Another difference detected between these C2 domains was the value of ΔC_p, which was higher for the PKCα−C2 domain than for the PKCβII− and PKCγ−C2 domains (Table 3). The increase in ΔC_p during unfolding is due to the change in the degree of exposure to the solvent of the different amino acidic residues (*40*, *50*, *76*−*79*), and it is clear that the PKCα−C2 domain suffers a bigger change in this sense than the other C2 domains.

The differences among the thermal stability of these C2 domains and the enhancement promoted by Ca^{2+} binding may reflect differences in the distribution of stability through the domain structure of the three isoenzymes, which, in turn, could be related to their distint functional roles. This may be an important factor when explaining their different capacities to act in very different environments, although it cannot be appreciated by high-resolution studies of the domain structure. In this sense, further studies are necessary to explain the relation between the behavior of the regulatory domains and the function of the full-length proteins.

The observations made in this paper are compatible with previous models (*80*, *81*) suggesting that the binding of Ca^{2+} to the C2 domain of inactive PKCα facilitates the binding of the protein to the membrane. It seems that the first Ca^{2+} is bound to the C2 domain with very high affinity, as seen

by ITC, and that the binding of two additional Ca^{2+} ions of lower affinity triggered an important structural stabilization, as detected by DSC. In addition, both ITC and DSC detected an enhancement of lipid binding mediated by Ca^{2+}, which reflects the triggering of membrane binding mediated by the C2 domains.

ACKNOWLEDGMENT

We thank Drs. Ono and Nishizuka (University of Kobe, Kobe, Japan) for the kind gift of the PKCα and PKCβII cDNAs and Dr. T. Meyer (Standford University Medical School, Standford, CA) for the PKCγ cDNA.

REFERENCES

1. Nishizuka, Y. (1988) The molecular heterogeneity of protein kinase C and its implications for cellular regulation, *Nature 334*, 661−665.
2. Bell, R. M., and Burns, D. J. (1991) Lipid activation of protein kinase C, *J. Biol. Chem. 266*, 4661−4664.
3. Newton, A. C. (1995) Protein kinase C: Structure, function, and regulation, *J. Biol. Chem. 270*, 28495−28498.
4. Mellor, H., and Parker, P. J. (1998) The extended protein kinase C superfamily, *Biochem. J. 332*, 281−292.
5. Hoffman, J. (1997) The potential for isoenzyme-selective modulation of protein kinase C, *FASEB J. 11*, 649−669.
6. Nishizuka, Y. (1995) Protein kinase C and lipid signaling for sustained cellular responses, *FASEB J. 9*, 484−496.
7. Newton, A. C., and Johnson, J. E. (1998) Protein kinase C: A paradigm for regulation of protein function by two membrane-targeting modules, *Biochim. Biophys. Acta 1376*, 155−172.
8. Edwards, A. S., and Newton, A. C. (1997) Regulation of protein kinase C βII by its C2 domain, *Biochemistry 36*, 15615−15623.
9. Medkova, M., and Cho, W. (1998) Mutagenesis of the C2 domain of protein kinase Cα. Differential roles of Ca^{2+} ligands and membrane binding residues, *J. Biol. Chem. 273*, 17544−17552.
10. Sutton, R. B., Davletov, B. A., Berghuis, A. M., Südhof, T. C., and Sprang, S. R. (1995) Structure of the first C2 domain of synaptotagmin I: A novel Ca^{2+}/phospholipid-binding fold, *Cell 80*, 929−938.
11. Shao, X., Fernandez, I., Sudhof, T. C., and Rizo, J. (1998) Solution structures of the Ca^{2+}-free and Ca^{2+}-bound C2A domain of synaptotagmin I: Does Ca^{2+} induce a conformational change? *Biochemistry 37*, 16106−16115.
12. Sutton, R. B., Ernst, J. A., and Brunger, A. T. (1999) Crystal structure of the cytosolic C2A−C2B domains of synaptotagmin III. Implications for Ca^{2+}-independent snare complex interaction, *J. Cell. Biol. 147*, 589−598.
13. Essen, L. O., Perisic, O., Cheung, R., Katan, M., and Williams, R. L. (1996) Crystal structure of a mammalian phosphoinositide-specific phospholipase C δ, *Nature 380*, 595−602.
14. Grobler, J. A., Essen, L. O., Williams, R. L., and Hurley, J. H. (1996) Catalysis by phospholipase C δ1 requires that Ca^{2+} bind to the catalytic domain, but not the C2 domain, *Nat. Struct. Biol. 3*, 788−795.
15. Perisic, O., Fong, S., Lynch, D. E., Bycroft, M., and Williams, R. L. (1998) Crystal structure of a calcium-phospholipid binding domain from cytosolic phospholipase A2, *J. Biol. Chem. 273*, 1596−1604.
16. Xu, G. Y., McDonagh, T., Yu, H. A., Nalefski, E. A., Clark, J. D., and Cumming, D. A. (1998) Solution structure and membrane interactions of the C2 domain of cytosolic phospholipase A2, *J. Mol. Biol. 280*, 485−500.
17. Dessen, A., Tang, J., Schmidt, H., Stahl, M., Clark, J. D., and Cumming, D. A. (1999) Crystal structure of human cytosolic phospholipase A2 reveals a novel topology and catalytic mechanism, *Cell 97*, 349−360.
18. Sutton, R. B., and Sprang, S. R. (1998) Structure of the protein kinase Cβ phospholipid-binding C2 domain complexed with Ca^{2+}, *Structure 6*, 1395−1405.
19. Pappa, H., Murray-Rust, J., Dekker, L. V., Parker P. J., and McDonald, N. Q. (1998) Crystal structure of the C2 domain from protein kinase C-δ. Crystal structure of the C2 domain from protein kinase C-δ, *Structure 6*, 885−894.
20. Verdaguer, N., Corbalán-García, S., Ochoa, W. F., Fita, I., and Gómez-Fernández, J. C. (1999) Ca^{2+} bridges the C2 membrane-binding domain of protein kinase Cα directly to phosphatidylserine, *EMBO J. 18*, 6329−6338.
21. Ochoa, W. F., Corbalán-García, S., Eritja, R., Rodríguez-Alfaro, J. A., Gómez-Fernández, J. C., Fita, I., and Verdaguer, N. (2002) Additional binding sites for anionic phospholipids and calcium ions in the crystal structures of complexes of the C2 domain of protein kinase Cα, *J. Mol. Biol. 320*, 277−291.
22. Ochoa, W. F., Torrecillas, A., Fita, I., Verdaguer, N., Corbalán-García, S., and Gómez-Fernández, J. C. (2003) Retinoic acid binds to the C2-domain of protein kinase Cα, *Biochemistry 42*, 8774−8779.
23. Ochoa, W. F., García-García, J., Fita, I., Corbalán-García, S., Verdaguer, N., and Gómez-Fernández, J. C. (2001) Structure of the C2 domain from novel protein kinase Cϵ. A membrane binding model for Ca^{2+}-independent C2 domains, *J. Mol. Biol. 311*, 837−849.
24. Lee, J. O., Yang, H., Georgescu, M. M., Di Cristofano, A., Maehama, T., Shi, Y., Dixon, J. E., Pandolfi, P., and Pavletich, N. P. (1999) Crystal structure of the PTEN tumor suppressor: Implications for its phosphoinositide phosphatase activity and membrane association, *Cell 99*, 323−334.
25. Walker, E. H., Perisic, O., Ried, C., Stephens, L., and Williams, R. L. (1999) Structural insights into phosphoinositide 3-kinase catalysis and signalling, *Nature 402*, 313−320.
26. Nalefski, E. A., and Falke, J. J. (1996) The C2 domain calcium-binding motif: Structural and functional diversity, *Protein Sci. 5*, 2375−2390.
27. Rizo, J., and Südhof, T. C. (1998) C2-domains, structure and function of a universal Ca^{2+}-binding domain, *J. Biol. Chem. 273*, 15879−15882.
28. Davletov, B. A., and Südhof, T. C. (1993) A single C2 domain from synaptotagmin I is sufficient for high affinity Ca^{2+}/phospholipid binding, *J. Biol. Chem. 268*, 26386−26390.
29. Li, C., Ullrich, B., Zhang, J. Z., Anderson, R. G. W., Bzor, N., and Südhof, T. C. (1995) Ca^{2+}-dependent and -independent activities of neural and non-neural synaptotagmins, *Nature 375*, 594−599.
30. Shao, X., Davletov, B. A., Sutton, R. B., Südhof, T. C., and Rizo, J. (1996) Bipartite Ca^{2+}-binding motif in C2 domains of synaptotagmin and protein kinase C, *Science 273*, 248−251.
31. Nalefski, E. A., Slazas, M. M., and Falke, J. J. (1997) Ca^{2+}-signaling cycle of a membrane-docking C2 domain, *Biochemistry 36*, 12011−12018.
32. Ohno, S., Akita, Y., Hata, A., Osada, S., Kubo, K., Konno, Y., Akimoto, K., Mizuno, K., Saido, T., Kuroki, T., and Suzuki, K. (1991) Structural and functional diversities of a family of signal transducing protein kinases, protein kinase C family; two distinct classes of PKC, conventional cPKC and novel nPKC, *Adv. Enzyme Regul. 31*, 287−303
33. Dempsey, E. C., Newton, A. C., Mochly-Rosen, D., Fields, A. P., Reyland, M. E., Insel, P. A., and Messing, R. O. (2000) Protein kinase C isozymes and the regulation of diverse cell responses, *Am. J. Physiol. Lung Cell. Mol. Physiol. 279*, L429−L438.
34. Nishizuka, Y. (1992) Intracellular signaling by hydrolysis of phospholipids and activation of protein kinase C, *Science 258*, 607−614.
35. Knopf, J. L., Lee, M.-H., Sultzman, L. A., Kriz, R. R. W., Loomis, C. R., Hewick, R. M., and Bell, R. M. (1986) Cloning and expression of multiple protein kinase C cDNAs, *Cell 46*, 491−502.
36. Ono, Y., Fujii, T., Igarashi, K., Kikkawa, U., Ogita, K., and Nishizuka, Y. (1988) Nucleotide sequences of cDNAs for α and γ subspecies of rat brain protein kinase C, *Nucleic Acids Res. 16*, 5199−5200.
37. Housey, G. M., Johnson, M. D., Hsiao, W. L., O'Brian, C. A., Murphy, J. P., Kirschmeier, P., and Weinstein, I. B. (1988) Overproduction of protein kinase C causes disordered growth control in rat fibroblasts, *Cell 52*, 343−354.
38. Kohout, S. C., Corbalán-García, S., Torrecillas, A., Gómez-Fernández, J. C., and Falke, J. J. (2002) C2 domains of protein kinase C isoforms α, β, and γ: Activation parameters and calcium stoichiometries of the membrane-bound state, *Biochemistry 41*, 11411−11424.
39. Torrecillas, A., Corbalán-García, S, and Gómez-Fernández, J. C. (2003) Structural study of the C2 domains of the classical PKC

isoenzymes using infrared spectroscopy and two-dimensional infrared correlation spectroscopy, *Biochemistry 42*, 11669−11681.
40. Jelesarov, I., and Bosshard, H. R. (1999) Isothermal titration calorimetry and differential scanning calorimetry as complementary tools to investigate the energetics of biomolecular recognition, *J. Mol. Recognit. 12*, 3−18.
41. Takahashi, K., and Fukada, H. (1985) Calorimetric studies of the binding of *Streptomyces* subtilisin inhibitor to subtilisin of *Bacillus subtilis* strain N′, *Biochemistry 24*, 297−300.
42. Shrake, A., and Ross, P. D. (1990) Ligand-induced biphasic protein denaturation, *J. Biol. Chem. 265*, 5055−5059.
43. Lin, L. N., Mason, A. B., Woodworth, R. C., and Brandts, J. F. (1994) Calorimetric studies of serum transferrin and ovotransferrin. Estimates of domain interactions, and study of the kinetic complexities of ferric ion binding, *Biochemistry 33*, 1881−1888.
44. Conejero-Lara, F., and Mateo, P. L. (1996) Presence of a slow dimerization equilibrium on the thermal unfolding of the 205−316 thermolysin fragment at neutral pH, *Biochemistry 35*, 3477−3486.
45. Grobler, J. A., and Hurley, J. H. (1998) Catalysis by phospholipase C δ1 requires that Ca^{2+} bind to the catalytic domain, but not the C2 domain, *Biochemistry 37*, 5020−5028.
46. Zheng, L., Krishnamoorthi, R., Zolkiewski, M., and Wang, X. (2000) Distinct Ca^{2+} binding properties of novel C2 domains of plant phospholipase D α and β, *J. Biol. Chem. 275*, 19700−19706.
47. García-García, J., Gómez-Fernández, J. C., and Corbalán-García, S. (2001) Structural characterization of the C2 domain of novel protein kinase Cϵ, *Eur. J. Biochem. 268*, 1107−1117.
48. García-García, J., Corbalán-García, S., and Gómez-Fernández, J. C. (1999) Effect of calcium and phosphatidic acid binding on the C2 domain of PKCα as studied by Fourier transform infrared spectroscopy, *Biochemistry 38*, 9667−9675.
49. Smith, P. K., Krohn, R. I., Hermanson, G. T., Mallia, A. K., Gartner, F. H., Provenzano, M. D., Fujimoto, E. K., Goeke, N. M., Olson, B. J., and Klenk, D. C. (1985) Measurement of protein using bicinchoninic acid, *Anal. Biochem. 150*, 76−85.
50. Laemmli, U. K. (1970) Cleavage of structural proteins during the assembly of the head of bacteriophage T4, *Nature 227*, 680−685.
51. Wiseman, T., Willinston, S., Brandts, J. F., and Lin, L. N. (1989) Rapid measurement of binding constants and heats of binding using a new titration calorimeter, *Anal. Biochem. 179*, 131−137.
52. Privalov, P. L., and Potekhin, S. A. (1986) Scanning microcalorimetry in studying temperature-induced changes in proteins, *Methods Enzymol. 131*, 4−51.
53. Sturtevant, J. M. (1987) Biochemical applications of differential scanning calorimetry, *Annu. Rev. Phys. Chem. 38*, 463−488.
54. Freire, E. (1995) Differential scanning calorimetry, *Methods Mol. Biol. 40*, 191−218.
55. Fabiato, A. (1988) Computer programs for calculating total from specified free or free from specified total ionic concentrations in aqueous solutions containing multiple metals and ligands, *Methods Enzymol. 157*, 378−417.
56. Freire, E., van Osdol, W. W., Mayorga, O., and Sánchez-Ruiz, J. M. (1990) Calorimetrically determined dynamics of complex unfolding transitions in proteins, *Annu. Rev. Biophys. Biophys. Chem. 19*, 159−188.
57. Sánchez-Ruiz, J. M. (1992) Theoretical analysis of Lumry−Eyring models in differential scanning calorimetry, *Biophys. J. 61*, 921−935.
58. Fukada, H., Sturtevant, J. M., and Quiocho, F. A. (1983) Thermodynamics of the binding of L-arabinose and of D-galactose to the L-arabinose-binding protein of *Escherichia coli*, *J. Biol. Chem. 258*, 13193−13198.
59. Jackson, M. B., and Sturtevant, J. M. (1978) Phase transitions of the purple membranes of *Halobacterium halobium*, *Biochemistry 17*, 911−915.
60. Brandts, J. F., and Lin, L. N. (1990) Study of strong to ultratight protein interactions using differential scanning calorimetry, *Biochemistry 29*, 6927−6940.
61. Basu, A. (1993) The potential of protein kinase C as a target for anticancer treatment, *Pharmacol. Ther. 59*, 257−280.
62. Ways, D. K., Kukoly, C. A., de Vente, J., Hooker, J. L., Bryant, W. O., Posekany, K. J., Fletcher, D. J., Cook, P. P., and Parker, P. J. (1995) MCF-7 breast cancer cells transfected with protein kinase C-α exhibit altered expression of other protein kinase C isoforms and display a more aggressive neoplastic phenotype, *J. Clin. Invest. 95*, 1906−1915.
63. Romanova, L. Y., Alexandrov, I. A., Schwab, G., Hilbert, D. M., Mushinski, J. F., and Nordan, R. P. (1996) Mechanism of apoptosis suppression by phorbol ester in IL-6-starved murine plasmacytomas: Role of PKC modulation and cell cycle, *Biochemistry 35*, 9900−9906.
64. Borner, C., Ueffing, M., Jaken, S., Parker, P. J., and Weinstein, I. B. (1995) Two closely related isoforms of protein kinase C produce reciprocal effects on the growth of rat fibroblasts. Possible molecular mechanisms, *J. Biol. Chem. 270*, 78−86.
65. Gokmen-Polar, Y., Murria, N. R., Velasco, M. A., Gatalica, Z., and Fields, A. P. (2001) Elevated protein kinase C βII is an early promotive event in colon carcinogenesis, *Cancer Res. 61*, 1375−1381.
66. Inoguchi, T., Battan, R., Handler, E., Sportsman, J. R., Heath, W., and King, G. L. (1992) Preferential elevation of protein kinase C isoform β II and diacylglycerol levels in the aorta and heart of diabetic rats: Differential reversibility to glycemic control by islet cell transplantation, *Proc. Natl. Acad. Sci. U.S.A. 89*, 11059−11063.
67. Frank, R. N. (2002) Potential new medical therapies for diabetic retinopathy: Protein kinase C inhibitors, *Am. J. Ophthalmol. 133*, 693−698.
68. Basbaum, A. I. (1999) Distinct neurochemical features of acute and persistent pain, *Proc. Natl. Acad. Sci. U.S.A. 96*, 7739−7743.
69. Martin, W. J., Malmberg, A. B., and Basbaum, A. I. (2001) PKCγ contributes to a subset of the NMDA-dependent spinal circuits that underlie injury-induced persistent pain, *J. Neurosci. 21*, 5321−5327.
70. Mazzoni, E., Adam, A., Bal de Kier Joffe, E., and Aguirre-Ghiso, J. A. (2003) Immortalized mammary epithelial cells overexpressing protein kinase C γ acquire a malignant phenotype and become tumorigenic in vivo, *Mol. Cancer Res. 1*, 776−787.
71. Sklyarova, T., De Corte, V., Meerschaert, K., Devriendt, L., Vanloo, B., Bailey, J., Cook, L. J., Goethals, M., Van Damme, J., Puype, M., Vandekerkhove, J., and Gettemans, J. (2002) Fragmin60 encodes an actin-binding protein with a C2 domain and controls actin Thr-203 phosphorylation in *Physarum* plasmodia and sclerotia, *J. Biol. Chem. 277*, 39840−39849.
72. Epand, R. F., Epand, R. M., and Jung, C. Y. (2001) Ligand-modulation of the stability of the glucose transporter GLUT 1, *Protein Sci. 10*, 1363−1369.
73. Shrake, A., and Ross, P. D. (1992) Origins and consequences of ligand-induced multiphasic thermal protein denaturation, *Biopolymers 32*, 925−940.
74. Edge, V., Allewell, N. M., and Sturtevant, J. M. (1985) High-resolution differential scanning calorimetric analysis of the subunits of *Escherichia coli* aspartate transcarbamoylase, *Biochemistry 24*, 5899−5906.
75. Hu, C. Q., and Sturtevant, J. M. (1989) A differential scanning calorimetric study of the binding of sulfate ion and of Cibacron blue F3GA to yeast phosphoglycerate kinase, *Biochemistry 28*, 813−818.
76. Sturtevant, J. M. (1977) Heat capacity and entropy changes in processes involving proteins, *Proc. Natl. Acad. Sci. U.S.A. 74*, 2236−2240.
77. Spolar, R. S., Ha, J. H., and Record, M. T. (1989) Hydrophobic effect in protein folding and other noncovalent processes involving proteins, *Proc. Natl. Acad. Sci. U.S.A. 86*, 8382−8385.
78. Privalov, P. L., and Makhatadze, G. I. (1990) Heat capacity of proteins. II. Partial molar heat capacity of the unfolded polypeptide chain of proteins: Protein unfolding effects, *J. Mol. Biol. 213*, 385−391.
79. Gómez, J., Hilser, V. J., Xie, D., and Freire, E. (1995) The heat capacity of proteins, *Proteins 22*, 404−412.
80. Medkova, M., and Cho, W. (1999) Interplay of C1 and C2 domains of protein kinase Cα in its membrane binding and activation, *J. Biol. Chem. 274*, 19852−19861.
81. Bolsover, S. R., Gómez-Fernández, J. C., and Corbalán-García, S. (2003) Role of the Ca^{2+}/phosphatidylserine binding region of the C2 domain in the translocation of protein kinase Cα to the plasma membrane, *J. Biol. Chem. 278*, 10282−10290.

BI0489659